

# Neutron scattering study of the field-induced soliton lattice in $\text{CuGeO}_3$

H. M. Rønnow<sup>1</sup>, M. Enderle<sup>2</sup>, D. F. McMorrow<sup>1</sup> L.-P. Regnault<sup>3</sup>,

G. Dhalle<sup>4</sup>, A. Revcolevschi<sup>4</sup>, A. Hoser<sup>5</sup>, K. Prokes<sup>5</sup>, P. Vorderwisch<sup>5</sup> and H. Schneider<sup>5</sup>

<sup>1</sup>Condensed Matter Physics and Chemistry Department, Risø National Laboratory, DK-4000 Roskilde, Denmark

<sup>2</sup>Univ. Saarlandes, Saarbrücken, Germany, <sup>3</sup>CENG, Grenoble, France, <sup>4</sup>Laboratoire de Chimie des Solides, Université de

Paris Sud, Orsay, France. <sup>5</sup>BENSC, Berlin, Germany

(August 10, 2018)

$\text{CuGeO}_3$  undergoes a transition from a spin-Peierls phase to an incommensurate phase at a critical field of  $H_c \approx 12.5$  T. In the high-field phase a lattice of solitons forms, with both structural and magnetic components, and these have been studied using neutron scattering techniques. Our results provide direct evidence for a long-ranged magnetic soliton structure which has both staggered and uniform magnetizations, and with amplitudes that are broadly in accord with theoretical estimates. The magnetic soliton width,  $\Gamma$ , and the field dependence of the incommensurability,  $\delta k_{\text{sp}}$ , are found to agree well with theoretical predictions.

A spin  $\frac{1}{2}$  antiferromagnetic (AF) chain in a deformable 3D lattice may, at a characteristic temperature  $T_{\text{sp}}$ , undergo a spin-Peierls transition into a correlated dimerized groundstate characterized by a total spin  $S_{\text{tot}} = 0$ . The energy cost of deforming the lattice is more than compensated for by the reduction in magnetic energy, and a gap opens in the magnetic excitation spectrum which reduces the influence of zero-point fluctuations [1]. This intriguing magneto-elastic phenomenon gives rise to several interesting properties. The groundstate is predicted to be a non-magnetic singlet separated from an excited triplet ( $S_{\text{tot}} = 1$ ) by a gap of energy  $\Delta_0 = 1.76 T_{\text{sp}}$ . The opening of this gap produces anomalies in the temperature dependence of physical quantities like the magnetic susceptibility, specific heat, etc. Dimerization also results in a doubling of the unit cell along the chain direction, which is reflected in diffraction experiments by the appearance of satellite reflections at commensurate, half-order positions.

Application of a magnetic field reduces the stability of the spin-Peierls (SP) state against a state with finite magnetization and, at a critical field  $H_c \simeq 0.84\Delta_0/g\mu_B$ , the system enters an incommensurate high-field phase [2,3]. Above  $H_c$ , the development of a uniform magnetization can be visualized as the breaking of a dimer bond, thus allowing two spins to become parallel to the magnetic field. The two  $S^z = \frac{1}{2}$  states can be regarded as a pair of domain walls with respect to the dimer order. The transverse part of the AF interaction delocalizes the domain walls into solitons of finite width  $\Gamma$ , and the longitudinal part causes the two domain walls to repel each other, thus forming an equally spaced lattice of solitons. The resulting soliton has both ferromagnetic and AF components and, in addition, the lattice distortion also becomes incommensurate. The average magnetization is proportional to the number of solitons, and inversely proportional to the separation  $L$ .

Theoretically, the coupling of the spin chains to the lattice is usually treated within the adiabatic approxima-

tion. A continuum model has been developed by applying bosonization techniques to the Jordan-Wigner transformed Hamiltonian [4]. This field-theoretical approach provides an analytic description of the soliton structure in terms of the soliton spacing,  $L/c = 1/\delta k_{\text{sp}}$ , soliton width,  $\Gamma$ , and the amplitudes of the uniform,  $m_{\text{u}}$ , and staggered,  $m_{\text{s}}$ , magnetizations [5–7]. The formalism has been extended to include next-nearest neighbour (nnn) and inter-chain interactions [8,9], but it is somewhat unclear to what extent the results are affected by the various approximations involved. Monte Carlo [10] and density matrix renormalization group (DMRG) calculations have also been performed [11,12]. While the soliton shape matches the field theoretical solution, the DMRG calculations show that the structural and magnetic soliton widths are in general different to each other and field dependent.

As the high-field soliton lattice has both a structural and magnetic component it is desirable to use a probe that is sensitive to both. In this letter we report the results of an investigation of the structure of the high-field phase of  $\text{CuGeO}_3$  using neutron scattering techniques.

Experimental investigations of the SP transition were initiated by the work of Bray *et al.* on the organic compound  $\text{TTFCuS}_4\text{C}_4(\text{CF}_3)_4$  [3]. Interest in SP systems intensified with the discovery by Hase *et al.* [13] that  $\text{CuGeO}_3$  undergoes an SP transition at  $T_{\text{sp}} = 14$  K.  $\text{CuGeO}_3$  crystallises in the orthorhombic  $Pbmm$  structure with room-temperature lattice parameters of  $a = 4.80$  Å,  $b = 8.47$  Å and  $c = 2.94$  Å, and the  $S = \frac{1}{2}$   $\text{Cu}^{2+}$  moments form chains along the  $c$ -axis. The field theory predictions depend on the spin gap  $\Delta_0 = 2$  meV and spin-wave velocity  $v_s = 16.6$  meV, which have been determined using inelastic neutron scattering [14–16]. The inter-chain couplings  $J_a = -0.08$  meV and  $J_b = 0.62$  meV indicate that the system is in fact only quasi-1D [17]. Along the chain, both an alternating exchange coupling  $J_c^\pm = (1 \pm 0.014) \times 14$  meV and a significant nnn coupling  $J'_c \simeq 0.35J_c$  are needed to model the suscepti-

bility, saturation field and excitation spectrum [18].

In zero-field the expected doubling of the unit cell along the  $c$  direction below  $T_{\text{SP}}$  has been confirmed by electron [19], X-ray [20] and neutron [21,22] diffraction experiments. The strongest satellite reflections appear at  $(\frac{h}{2}, k, \frac{l}{2})$  with  $h, k$  and  $l$  odd, which indicates that along  $a$  and  $b$  adjacent chains dimerize in anti-phase. Hirota *et al.* [21] and Braden *et al.* [22] have solved the detailed structure of the SP phase, which is characterized by the propagation wavevector  $k_{\text{SP}} = (\frac{1}{2}, 0, \frac{1}{2})$  and three displacement parameters:  $u_c^{\text{Cu}}/c = 0.00192$ ,  $u_a^{\text{O}2}/a = 0.00198$ ,  $u_b^{\text{O}2}/b = 0.00077$ .

Several experiments have been reported on the high-field phase, including X-ray scattering [23], thermal expansion [24], FIR spectroscopy [25], NMR [26], ESR and magnetization [27,28]. The predicted incommensurability of the structure was observed in an X-ray experiment [23] as a splitting of the satellite reflection into  $(\frac{7}{2}, 1, \frac{5}{2} \pm \delta k_{\text{SP}})$ , and the soliton width was estimated to be  $\Gamma = (13.6 \pm 0.3)c$ . Using copper NMR, Horvatić *et al.* [26] have determined the staggered and uniform magnetizations to be  $m_s = 0.026$  and  $m_u = 0.023$ , respectively at 14.5 T. (By definition a spin of  $\frac{1}{2}$  corresponds to  $m = \frac{1}{2}$ .) Magnetization measurements give a value of 0.018 for  $m_u$ . The theoretical values are  $m_s = 0.11 \leftrightarrow 0.14$  and  $m_u = 0.023$  [5–9,12]. Thus although there is good agreement between theory and experiment for  $m_u$ , the staggered moment observed in NMR is significantly lower than the theoretical value, a point we will return to later.

Although neutron scattering is an obvious way to attempt to study the magnetic soliton lattice, it has until recently not been possible to apply this technique above 12 T. In  $\text{CuSi}_{0.03}\text{Ge}_{0.97}\text{O}_3$ , where  $H_c$  is reduced to 11.7 T, Grenier *et al.* [29] have measured the intensity of five satellite reflections upon entering the high-field phase. No clear evidence of any magnetic scattering was found. The soliton width at 12 T was deduced to be  $13.5c$ , in agreement with the X-ray data on pure  $\text{CuGeO}_3$ .

Here, we report on a neutron scattering study of the high-field phase in pure  $\text{CuGeO}_3$ , performed at HMI, Berlin, using a 14.5 T vertical field cryomagnet with a base temperature of 1.6 K. The single crystal of dimensions  $3 \times 7 \times 16 \text{ mm}^3$  was grown by the floating zone method. In total three different instruments were used, each chosen to reveal a particular aspect of the phase transition. Due to the slightly anisotropic  $g$ -tensor [30], the critical field depends on the orientation of the applied magnetic field.

The field dependence of the incommensurability was investigated using the thermal triple-axis spectrometer E1 with a collimation of  $20^\circ\text{-}40^\circ\text{-}20^\circ\text{-}80^\circ$ , and a wavelength of  $\lambda = 2.425 \text{ \AA}$ . By performing scans along  $c^*$  through five satellite reflections  $(\frac{1}{2}, 1, \frac{1}{2})$ ,  $(\frac{1}{2}, 3, \frac{1}{2})$ ,  $(\frac{3}{2}, 3, \frac{1}{2})$ ,  $(\frac{1}{2}, 1, \frac{3}{2})$  and  $(\frac{1}{2}, 3, \frac{3}{2})$ , we observed the expected splitting.

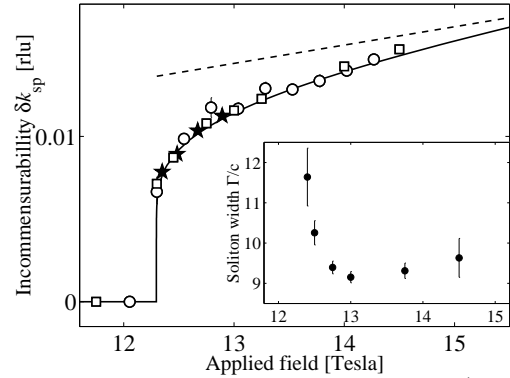


FIG. 1. The measured splitting  $\delta k_{\text{SP}}$  of  $(\frac{1}{2}, 1, \frac{1}{2})$  ( $\square$ ) and  $(\frac{1}{2}, 3, \frac{1}{2})$  ( $\circ$ ), compared to X-ray data [23] ( $\star$ ), and to the theories of Cross and Fisher [2] (dashed line), and Buzdin *et al.* [6] (solid line with  $\Delta_0/v_s = 0.13$ ). For clarity, only a representative selection of the X-ray data is shown, and all of the data has been scaled to the  $g$  factor corresponding to the  $(h, 2h, l)$  orientation. The insert shows the soliton width  $\Gamma$  as obtained from the relative intensity of the 3rd harmonics.

As shown in Fig. 1, the field dependence of  $\delta k_{\text{SP}}$  is consistent with the X-ray results in the region of overlap, but our data extend to much higher fields. Field theory [6] predicts that the incommensurability of the soliton lattice is given by  $1/\delta k_{\text{SP}} = \frac{2v_s}{\Delta_0} \ln \frac{8H_c}{H-H_c}$ . Using the upper limit value of 0.13 for the experimentally determined ratio  $\Delta_0/v_s = 0.12 \pm 0.01$ , we obtain perfect agreement with our data. At the highest fields, the linear field dependence  $\delta k_{\text{SP}} = g\mu_B H / (2\pi v_s)$  is approached [2].

One striking feature of this data set is that there was a tremendous increase in intensity of the low  $Q$  satellites. This appears difficult to explain on the basis of a purely structural distortion, for which the intensity increases in proportion to  $Q^2$ . One possible explanation could be that the magnetic soliton lattice has the same propagation vector as the lattice soliton. At first sight this seems unlikely, as the minimum energy gap in the spin-wave spectrum is located at  $(0, 1, \frac{1}{2})$ , which is also the propagation vector of the AF structure found in doped systems [31]. It should be noted, however, that the magnetic coupling in the  $a$  direction is weak, of order 1 K, and could be overcome by stronger lattice forces. To exclude the possibility that there is magnetic scattering from the staggered component at wavevectors other than  $(\frac{h}{2}, k, \frac{l}{2})$ , an exhaustive search for additional satellite reflections that may be associated with long range magnetic order was conducted. From this an upper limit can be put on any Fourier component at  $(0, 1, \frac{1}{2})$ ,  $(0, 3, \frac{1}{2})$  and  $(0, 0, \frac{1}{2})$  of  $0.005\mu_B$  at 14.5 T.

To investigate whether in fact there is a magnetic contribution to the low- $Q$  satellites, a second experiment was undertaken. The two-axis spectrometer E4 was used with a collimation of  $40^\circ\text{-}40^\circ\text{-}40^\circ$  and  $\lambda = 1.2205 \text{ \AA}$ , which made 14 satellite reflections accessible in the  $(h, 2h, l)$ -

plane (see Table I). Rocking curves of each reflection were collected at 2 K in zero field and 14.5 T. An additional data set was taken at 20 K (above  $T_{\text{SP}} = 14.1$  K) and 0 T to determine the  $\lambda/2$  contamination. The widths of all measured peaks were in complete agreement with an analytic resolution calculation, and this was used to correct the integrated intensities of the measured satellite peaks. The overall scale factor that converts the satellite intensities to structure factors can be found by accurately determining the structure factors of the main Bragg peaks. However, this process is often problematic, as it involves additional corrections for extinction, absorption, and in our case  $\lambda/2$  contamination. To avoid these problems, we chose instead an overall scale factor such that the sum of the displacement parameters obtained when fitting our zero-field data matched the sum of the parameters obtained in the detailed study by Braden *et al.* [22]. The relative size of our zero-field displacement parameters  $u_z^{\text{Cu}}/c = 0.00204 \pm 0.00014$ ,  $u_x^{\text{O}2}/a = 0.00182 \pm 0.00010$  and  $u_y^{\text{O}2}/b = 0.00079 \pm 0.00009$  agree well with the values reported by Braden *et al.*

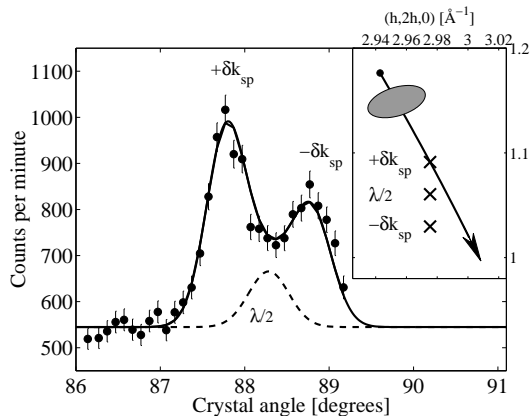


FIG. 2. Rocking curve through  $(\frac{3}{2}, 3, \frac{1}{2} + \delta k_{\text{sp}})$  at 14.5 T, 2 K. The finite instrument resolution picks up both satellites  $(\frac{3}{2}, 3, \frac{1}{2} + \delta k_{\text{sp}})$ , and the  $\lambda/2$  background at  $(\frac{3}{2}, 3, \frac{1}{2})$ . The solid line shows a fit of three resolution convoluted peaks. The insert displays the reciprocal space trajectory of the scan and the resolution ellipse. The position of each peak is marked with a cross.

The same scale factor was used for the data taken in the high-field phase at 14.5 T (Table I). The resolution obtainable with the short wavelength was insufficient to completely separate the two satellites  $(\frac{h}{2}, h, \frac{l}{2} \pm \delta k_{\text{sp}})$  and the  $\lambda/2$  background at all  $(\frac{h}{2}, h, \frac{l}{2})$ . This is illustrated in the scan through  $(\frac{3}{2}, 3, \frac{1}{2} + \delta k_{\text{sp}})$  shown in Fig. 2. The data were fitted to three peaks convoluted with the calculated resolution. The  $\lambda/2$  contribution was fixed to the value determined at 20 K and 0 T, and the two satellites were given equal amplitude. With the satellite amplitude as the only fitting parameter, all fourteen reflections gave excellent fits as shown by the solid line in Fig. 2. The resulting structure factors are listed in Table I.

$2h$	$k$	$2l$	0 T		14.5 T	
			$ F _{\text{exp}}^2$	$ F _{\text{fit}}^2$	$ F _{\text{exp}}^2$	$ F _{\text{fit}}^2$
1	1	1	$4 \pm 1$	1	$40 \pm 1$	41
3	3	1	$3 \pm 2$	1	$31 \pm 1$	29
1	1	3	$26 \pm 5$	16	$33 \pm 1$	30
3	3	3	$36 \pm 3$	34	$29 \pm 3$	26
5	5	1	$30 \pm 4$	20	$16 \pm 1$	21
1	1	5	$35 \pm 11$	34	$14 \pm 5$	20
5	5	3	$83 \pm 4$	89	$30 \pm 2$	28
3	3	5	$18 \pm 6$	16	$12 \pm 2$	15
7	7	1	$86 \pm 8$	90	$25 \pm 5$	37
5	5	5	$13 \pm 8$	0	$10 \pm 1$	9
1	1	7	$89 \pm 10$	81	$16 \pm 2$	21
7	7	3	$218 \pm 14$	208	$87 \pm 7$	59
3	3	7	$85 \pm 17$	116	$28 \pm 3$	25
7	7	5	$25 \pm 32$	21	$0 \pm 7$	17
$\chi^2$			2.8		6.5	

TABLE I. Measured and fitted structure factors in units of  $10^{-27} \text{ cm}^{-2}$ .

As anticipated, it was not possible to obtain satisfactory fits of the high-field structure factors by assuming a structural distortion alone. Instead, a magnetic Fourier component of variable size and direction with the magnetic form-factor of  $\text{Cu}^{2+}$  was included in the fit. The resulting displacement parameters  $u_z^{\text{Cu}}/c = 0.00158 \pm 0.00026$ ,  $u_x^{\text{O}2}/a = 0.00196 \pm 0.00036$  and  $u_y^{\text{O}2}/b = 0.00061 \pm 0.00025$  are not significantly different from the zero field parameters. The direction of the magnetic moments was found to be parallel/antiparallel to the field, in agreement with theoretical expectations. The Fourier component was determined to be  $\mu(q = \delta k_{\text{sp}}) = 0.098 \pm 0.003 \mu_B$  at 14.5 T.

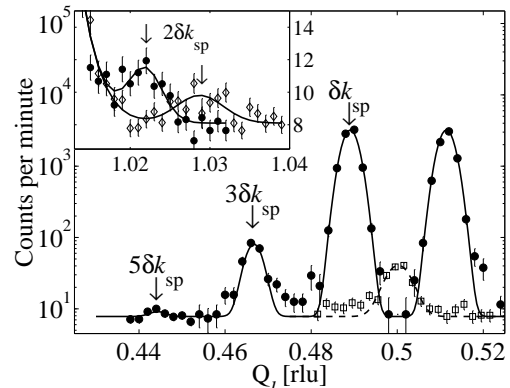


FIG. 3. Scans along  $[00l]$  through  $(\frac{1}{2}, 1, \frac{1}{2})$  at 1.6 K and 0 T (squares), and 13 T (filled circles). The resolution limited peaks were fitted to Gaussian line shapes. The higher harmonics  $n\delta k_{\text{sp}}$  are marked by arrows. The insert shows scans through  $(0, 0, 1 + 2\delta k_{\text{sp}})$  at 13 T (filled circles) and 14.5 T (diamonds).

Having established that the  $(\frac{1}{2}, 1, \frac{1}{2} \pm \delta k_{\text{sp}})$  reflection is almost completely magnetic in origin, we performed

a high-resolution experiment in order to investigate the detailed structure of the magnetic soliton lattice. Using the cold triple axis spectrometer V2 with  $\lambda = 5.236 \text{ \AA}$  and 20' collimation gave a resolution of  $0.009 \text{ \AA}^{-1}$ . Fig. 3 shows scans through  $(\frac{1}{2}, 1, \frac{1}{2})$  along  $[00l]$  at 0 T and at 13 T. Along with the dramatic increase in intensity, the 13 T scan reveals both third and fifth harmonics, which reflect the non-sinusoidal shape of the magnetic solitons.

From field theory, an analytical solution for the magnetization  $\langle S^z(l) \rangle = m_s(-1)^l \text{cn}(lc/\Gamma k, k) + m_u \text{dn}(lc/\Gamma k, k)$  at site  $l$  with amplitudes  $m_s = \sqrt{\frac{\Delta_0}{2\pi v_s}}$  and  $m_u = \frac{\Delta_0}{2\pi k v_s}$  is given in terms of the Jacobian elliptic functions cn and dn of modulus  $k$ , where  $L/\Gamma = 4kK(k)$  and  $K(k)$  is the complete elliptic integral of first kind [5–8]. The  $n$ th Fourier components of the staggered and uniform parts of the magnetic structure are given by  $\frac{\pi}{kK(k)} \frac{\kappa^{n/2}}{1+\kappa^n}$  ( $n$  odd) and  $\frac{\pi}{K(k)} \frac{\kappa^{n/2}}{1+\kappa^n}$  ( $n > 0$  even) respectively, where  $\kappa = e^{-\pi K(\sqrt{1-k^2})/K(k)}$ . From the ratio  $\kappa^2/(1-\kappa+\kappa^2)^2$  between the intensities of the third and the first harmonic, we determine the modulus  $k$  and the soliton width  $\Gamma/c = 1/(4\delta k_{\text{sp}} k K(k))$ , which is shown in the insert of Fig. 1. Above the transition,  $\Gamma/c$  quickly decreases from 11.5 to a value of 9, followed by a slight increase with field, a feature which is also apparent in DMRG calculations [12]. Except for the rapid change just above  $H_c$ , our data are in fair agreement with the constant value  $\Gamma/c = v_s/\Delta = 8.3$  predicted by field theory, but differs from the values  $\Gamma/c \sim 13.5$  obtained from X-ray and neutron scattering on the Si doped system. We believe that this is because the latter experiments measure the width of the structural soliton, which in the presence of nnn coupling is larger than the magnetic soliton width [12]. Re-analysing the X-ray data, by allowing for a field dependent soliton width, leads to a similar decrease  $\Gamma/c = 15.1 \rightarrow 12.9$  with increasing field.

Knowing the precise soliton shape, the amplitude of the staggered moment can be determined from the Fourier component:  $m_s = \frac{kK(k)}{\pi} \frac{1+\kappa}{\sqrt{\kappa}} \frac{\mu(q=\delta k_{\text{sp}})}{g} = 0.097 \pm 0.003$ , where  $g = 2.19$  for  $B \perp (h, 2h, l)$  [30]. This value is in reasonable agreement with theoretical estimates cited earlier, but is considerably larger than the value derived from NMR. If, as has been suggested, the NMR value is reduced by quantum fluctuations in the groundstate [26,12], then these would also reduce the value of  $m_s$  observed in our neutron scattering experiments. The NMR and neutron scattering data can be reconciled if there are fluctuations fast compared to the time scale probed by NMR ( $\sim 10^{-4}$  THz) but slow compared to that probed by the neutron scattering ( $\sim$ THz).

The uniform part of the magnetic structure should give rise to even harmonics around integer positions in reciprocal space. Indeed, second-order harmonics were found near the (0,0,1) Bragg reflection, as shown in the insert of Fig. 3. To extract the absolute structure factor, we scale

the integrated intensity to the  $(\frac{1}{2}, 1, \frac{1}{2} \pm \delta k_{\text{sp}})$  reflection measured in the same configuration, correcting for the different resolution volumes. The resulting Fourier component of the magnetic structure is  $\mu(0, 0, 1 + 2\delta k_{\text{sp}}) = 0.0046\mu_B$  at 14.5 T. The amplitude of the uniform component is then given by  $m_u = \frac{K(k)}{\pi} \frac{1+\kappa^2}{\kappa} \frac{\mu(q=2\delta k_{\text{sp}})}{g} = 0.019 \pm 0.003$ , about 25% lower than the field theory and NMR results. It should be noted that although the individual values of  $m_s$  and  $m_u$  are sensitive to the details of any normalisation procedure, the ratio  $m_s/m_u = 5.1 \pm 0.8$  is not, and is seen to be in good agreement with the theoretical ratio  $m_s/m_u = 5.4$ .

In summary, neutron scattering has been used to determine the nature of the soliton lattice in the high-field phase of the spin-Peierls compound  $\text{CuGeO}_3$ . The results provide a detailed description of the soliton lattice in terms of incommensurability,  $\delta k_{\text{sp}}$ , soliton width,  $\Gamma$ , and the amplitudes  $m_s$  and  $m_u$  of both the staggered and uniform parts of the magnetization.

We wish to thank R. A. Cowley, B. Keimer, B. Lebeck, K. Lefmann, B. Lake and V. J. Emery for valuable discussions, M. Meissner and P. Smeibidl for handling the cryomagnet. The experiments were performed at the HMI, Berlin with support from EC through TMR–LSF contract ERBFMGECT950060. We acknowledge support for HMR from the Danish Research Academy and for ME from BMBF.

- 
- [1] E. Pytte, Phys. Rev. B **10**, 4637 (1974).
  - [2] M. C. Cross and D. S. Fisher, Phys. Rev. B **19**, 402 (1979). *ibid* **20**, 4606 (1979).
  - [3] J. W. Bray *et al.*, in *Extended Linear Chain Compounds*, edited by J. S. Miller (Plenum, New York, 1983), p. 353.
  - [4] I. Affleck, in *Fields, Strings and Critical Phenomena*, edited by E. Brézin and J. Zinn-Justin (North-Holland, Amsterdam, 1990), p. 563.
  - [5] T. Nakano and H. Fukuyama, J. Phys. soc. Jpn. **49**, 1679 (1980). *ibid* **50**, 2489 (1981).
  - [6] A. I. Buzdin *et al.*, Solid State Comm. **48**, 483 (1983).
  - [7] M. Fujita and K. Machida, J. Phys. soc. Jpn. **53**, 4395 (1984).
  - [8] J. Zang *et al.*, Phys. Rev. B **55**, R14705 (1997).
  - [9] A. Dobry and J. Riera, Phys. Rev. B **56**, R2912 (1995).
  - [10] A. E. Feiguin *et al.*, Phys. Rev. B **56**, 14607 (1997).
  - [11] Y. Meurdesoif and A. Buzdin, Phys. Rev. B **59**, 11165 (1999).
  - [12] G. S. Uhrig *et al.*, Phys. Rev. B **60**, 9468 (1999).
  - [13] M. Hase *et al.*, Phys. Rev. Lett. **70**, 3651 (1993).
  - [14] M. Nishi *et al.*, Phys. Rev. B **50**, 6508 (1994).
  - [15] L. P. Regnault *et al.*, Phys. Rev. B **53**, 5579 (1996).
  - [16] The spin-wave velocity  $v_s$  is defined such that the dispersion follows  $\hbar\omega(q) = \sqrt{\Delta_0 + (v_s q)^2}$ , and its value is uniquely determined from neutron scattering data [15].

- [17] R. A. Cowley *et al.*, J. Phys. C **8**, L179 (1996). We have included the measured dispersion along  $a$  [15] in the determination of the coupling parameters.
- [18] J. Riera and A. Dobry, Phys. Rev. B **51**, 16098 (1995).
- [19] O. Kamimura *et al.*, J. Soc. Phys. Jpn. **63**, 2467 (1994).
- [20] J. P. Pouget *et al.*, Phys. Rev. Lett. **72**, 4037 (1994).
- [21] K. Hirota *et al.*, Phys. Rev. Lett. **73**, 736 (1994).
- [22] M. Braden *et al.*, Phys. Rev. B **54**, 1105 (1996).
- [23] V. Kiryukhin *et al.*, Phys. Rev. B **54**, 7269 (1996).
- [24] T. Lorenz *et al.*, Phys. Rev. Lett. **81**, 148 (1998).
- [25] P. H. M. van Loosdrecht *et al.*, Phys. Rev. B **54**, R3730 (1996).
- [26] M. Horvatić *et al.*, Phys. Rev. Lett. **83**, 420 (1999).
- [27] T. M. Brill *et al.*, Phys. Rev. Lett. **73**, 1545 (1994).
- [28] H. Hori *et al.*, Physica B **211**, 180 (1995).
- [29] B. Grenier *et al.*, Europhys. Lett. **44**, 511 (1998).
- [30] B. Pilawa, J. Phys. C **9**, 3779 (1997).
- [31] J. G. Lussier *et al.*, J. Phys. C **7**, L325 (1995).